Science of the Total Environment 912 (2024) 169264

Contents lists available at ScienceDirect

Science of the Total Environment

journal homepage: www.elsevier.com/locate/scitotenv

In the presence of the other: How glyphosate and peptide molecules alter the dynamics of sorption on goethite

Behrooz Azimzadeh [a], Linda K. Nicholson [b], Carmen Enid Martínez [a,*]

[a] Soil and Crop Sciences, School of Integrative Plant Science, Cornell University, Ithaca, NY 14853, USA
[b] Department of Molecular Biology and Genetics, Cornell University, Ithaca, NY 14853, USA

HIGHLIGHTS

- Glyphosate and the peptide do not interact in solution or at the goethite surface.
- Competition for the interface results in co-sorption of glyphosate and peptide.
- Outer-sphere glyphosate-goethite complexes are favored in the presence of peptide.
- Glyphosate reduces the extent and kinetics of peptide sorption onto goethite.
- Peptide reduces the extent while accelerating the kinetics of glyphosate sorption.

GRAPHICAL ABSTRACT

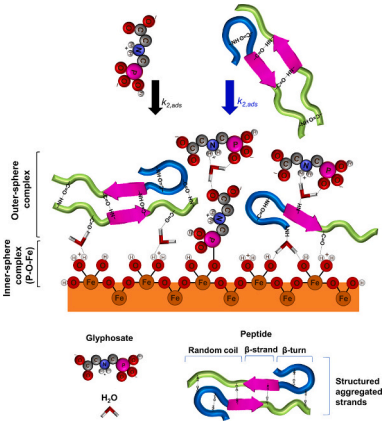

ARTICLE INFO

Editor: Baoliang Chen

Keywords:
Competition
Organo-mineral interactions
Glyphosate
Hydrogen bonds
Electrostatic interactions
Peptide conformation

ABSTRACT

The interactions with soil mineral surfaces are among the factors that determine the mobility and bioavailability of organic contaminants and of nutrients present in dissolved organic matter (DOM) in soil and aquatic environments. While most studies focus on high molar mass organic matter fractions (e.g., humic and fulvic acids), very few studies investigate the impact of DOM constituents in competitive sorption. Here we assess the sorption behavior of a heavily used herbicide (i.e., glyphosate) and a component of DOM (i.e., a peptide) at the water/goethite interface, inclusive of potential glyphosate-peptide interactions. We used *in-situ* ATR-FTIR (attenuated total reflectance Fourier-transform infrared) spectroscopy to study sorption kinetics and mechanisms of interaction as well as conformational changes to the secondary structure of the peptide. NMR (nuclear magnetic resonance) spectroscopy was used to assess the level of interaction between glyphosate and the peptide and changes to the peptide' secondary structure in solution. For the first time, we illustrate competition for sorption sites results in co-sorption of glyphosate and peptide molecules that affects the extent, kinetics, and mechanism of interaction of each with the surface. In the presence of the peptide, the formation of outer-sphere glyphosate-goethite complexes is favored albeit inner-sphere glyphosate-goethite bonds (i.e., P—O—Fe) are still formed. The

* Corresponding author at: Soil and Crop Sciences, School of Integrative Plant Science, College of Agriculture and Life Sciences, Cornell University, Ithaca, NY 14853, USA.
E-mail address: cem20@cornell.edu (C.E. Martínez).

https://doi.org/10.1016/j.scitotenv.2023.169264
Received 14 June 2023; Received in revised form 19 November 2023; Accepted 8 December 2023
Available online 11 December 2023

presence of glyphosate induces secondary structural shifts of the sorbed peptide that maximizes the formation of H-bonds with the goethite surface. However, glyphosate and the peptide do not seem to interact with one another in solution nor at the goethite surface upon sorption. The results of this work highlight potential consequences of competition for sorption sites, for example the transport of organic contaminants and nutrient-rich (i.e., nitrogen) DOM components in relevant environmental systems. Predicting the rate and extent with which organic pollutants are removed from solution by a given solid is also one of the most critical factors for the design of effective sorption systems in engineering applications.

1. Introduction

Glyphosate is the world's most heavily applied herbicide (Franz et al., 1997); as a result, contamination with glyphosate occurs frequently in a large variety of terrestrial environments (Aparicio et al., 2013; Avigliano and Schenone, 2015; Battaglin et al., 2005; Battaglin et al., 2014; Kolpin et al., 2006; Mahler et al., 2017; Primost et al., 2017; Richards et al., 2018; Skark et al., 1998). Detection of glyphosate in soil solution, surface water and groundwater occurs despite its (bio)degradation and sorption in soil. Since the dissolved organic matter (DOM) component of soil can mediate the transport of contaminants and nutrients to the subsurface, rivers and lakes (Daouk et al., 2015; Kaiser and Kalbitz, 2012; Qualls et al., 1991), detection of glyphosate could result from its competition with DOM components for mineral surfaces present within the soil matrix (Kalbitz et al., 2005).

DOM components of soil are chemically diverse, relatively small organic molecules (< ~3 kDa) of plant and microbial origin that include organic acids and biopolymer-derived organics (e.g., sugars, amino acids, polyphenols, peptides) (Ellert and Gregorich, 1995; Ladd et al., 2019; Roth et al., 2019; Sutton and Sposito, 2005; Van Hees et al., 2005; Warren, 2021). Peptides are protein-derived DOM components of varying composition and structure, produced by biotic and abiotic depolymerization and hydrolysis processes (Chalot and Brun, 1998; Hill et al., 2011; Jan et al., 2009; Ladd and Butler, 1972; Nguyen et al., 2019; Reardon et al., 2016; Vranova et al., 2013; Warren, 2021). Reactive metal oxide mineral surfaces (e.g., birnessite) can also induce chemical alterations to sorbed proteins and produce soluble peptides (Reardon et al., 2016; Russo et al., 2009).

Glyphosate reacts with soils (Glass, 1987; Hance, 1976; Pessagno et al., 2005) through its adsorption onto aluminosilicate clays (Damonte et al., 2007; Glass, 1987; Khoury et al., 2010; McConnell and Hossner, 1989; Morillo et al., 1997; Shoval and Yariv, 1979), birnessite (Li et al., 2018), and goethite (Barja and dos Santos Afonso, 2005; McBride and Kung, 1989), which potentially decreases its mobility and efficacy as a herbicide. Reports that evaluate the molecular-scale structures of glyphosate sorbed onto goethite generally show the formation of inner-sphere complexes (i.e., direct chemical bonds) through the phosphonate group of glyphosate (Barja and dos Santos Afonso, 2005; Jonsson et al., 2008; Sheals et al., 2002; Tribe et al., 2006; Yan and Jing, 2018) and outer-sphere complexes (e.g., electrostatic, H-bond interactions) through its carboxylate and/or amine groups (Azimzadeh and Martínez, 2024; Yan and Jing, 2018). Research also suggests glyphosate interacts with organic matter (OM); however, it is generally perceived that reactions between OM and organic pollutants are mostly driven by weak forces, such as hydrophobic interactions and hydrogen bonds (Kohl and Rice, 1998). Yet, interactions between glyphosate and soil humic acid extracts were found to be strong, thereby suggesting reactions with relatively large organic molecules might be important (Albers et al., 2009; Piccolo and Celano, 1994). Indeed, Mazzei and Piccolo (2012) reported the formation of H-bonds between glyphosate' carboxyl and phosphonate groups and protonated O-functionalities of extracted humic substances 5–10 kDa in mass. Spectroscopic studies have also shown the apparent disaggregation of humic molecules in the presence of glyphosate, possibly due to H-bond interactions between the phosphono group of glyphosate and the humic polymer (Miano et al., 1992). While the abovementioned studies suggest glyphosate interacts with relatively large OM fractions, quantum chemical modeling illustrates the potential for interactions between glyphosate and small DOM components. Ahmed et al. (2018) for example, predicted glyphosate and pentaglycine form a stable soluble complex (1:1 molar ratio) involving multiple intermolecular H-bonds, three with the phosphonic and one with the carboxylic group of glyphosate. If confirmed experimentally, these types of interactions are likely to be affected by the amino acid sequence of the peptide.

The adsorption of biomolecules onto mineral surfaces may be driven by several forces, including hydrogen bonding, ion exchange, ligand exchange, and electrostatic, hydrophobic and van der Waals interactions (Norde, 1996; Schmidt and Martínez, 2016; Schmidt and Martínez, 2017; Touzeau et al., 2021; Yang et al., 2022; Yang et al., 2021; Yu et al., 2013; Zhou et al., 2005). Properties that affect the sorption of biomolecules onto minerals include pH, ionic strength, the electrostatic properties of the surface, and the biomolecule' hydrophilic and hydrophobic character, functionality and molecular size (Norde, 1996; Touzeau et al., 2021; Yang et al., 2022; Yang et al., 2021). Structural investigations of peptide-surface associations are however scarce and mostly conducted at gold (Au), TiO_2, and SiO_2 surfaces. For example, Touzeau et al. (2021) show sorption of a peptidomimetic polymer on Au and hydrophilic TiO_2 and SiO_2 surfaces share a common mechanism involving initial electrostatic interactions followed by a sorption process driven by the increase in contacts on the surface where water displacement (i.e., entropic desolvation) plays a role. Additional studies have demonstrated a peptide derived from *Pseudomonas aeruginosa* has a higher affinity for hydrophobic than for hydrophilic surfaces (Yang et al., 2022; Yang et al., 2021). Overall, peptide sorption seems influenced not only by the peptide sequence, but also by the peptide conformation, which changes upon sorption (Touzeau et al., 2021; Yang et al., 2022; Yang et al., 2021).

It has been demonstrated that solution-phase interactions between high molecular mass organic molecules influence their sorption process (Schmidt and Martínez, 2018; Shakiba et al., 2018) and that humic acid and polysaccharide pre-sorbed onto goethite significantly reduce the extent and rate of glyphosate sorption compared to that on bare goethite (Arroyave et al., 2016; Azimzadeh and Martínez, 2024). Studies where both glyphosate and DOM were present in initial solutions have also shown glyphosate sorption onto goethite was significantly reduced by DOM at pH 3–9 (Day et al., 1997), thus suggesting DOM components might have a greater affinity for the goethite surface than glyphosate. It is therefore likely DOM modulates glyphosate sorption onto goethite by competition for surface sorption sites and that competition is determined by electrostatic and perhaps steric shielding effects (Day et al., 1997). To the best of our knowledge, no study to date has been conducted to investigate co-sorption of glyphosate and a low molar mass DOM component (e.g., peptide) at a mineral surface (e.g., goethite) and their solution-phase interactions.

We therefore investigate whether a peptide in solution - used as a model biomolecule component of DOM - hinders, facilitates, or competes with glyphosate for retention at a model mineral surface - goethite. The overarching question is *Do biomolecules present in the soil aqueous phase (components of DOM) outcompete glyphosate for retention at mineral surfaces?* Moreover, our experiments provide insights into the effects the addition of organic chemical contaminants to soils might have on soil dissolved organic matter components and hence on nutrient availability.

Experimentally, we investigate the extent and kinetics of sorption, and the mechanisms of interaction of glyphosate and the peptide from single (glyphosate or peptide) and binary (glyphosate + peptide) solutions at the goethite interface using *in-situ* ATR-FTIR spectroscopy in real time. Furthermore, NMR spectroscopy is used to assess whether glyphosate and the peptide interact in solution. In addition, we probe whether the peptide changes its conformation upon sorption in the presence and absence of glyphosate. Sorption to mineral surfaces is a significant factor that modulates the abiotic cycling of contaminants and nutrients (e.g., C and N in peptide) in terrestrial ecosystems and their availability to living organisms.

2. Experimental section

2.1. Materials

Goethite (α-FeOOH, $pH_{pzc} = 8.4 \pm 0.2$) (Azimzadeh and Martínez, 2024) was synthesized by the method of Schwertmann and Cornell (2008) which involves the addition of KOH to a $FeCl_3$ solution, followed by heating at 70 °C for 3 days, and purification of the suspension. Fig. S1 shows a SEM image of the synthesized product, with average length of needle-like crystals of 0.85 ± 0.4 μm and BET determined surface area of 59.1 ± 2.1 m^2 g^{-1}. Glyphosate (*N*-phosphonomethyl glycine, 96 % purity) was purchased from Sigma-Aldrich (Milwaukee, USA). The peptide, which is blocked at both ends, corresponds to amino acid residues 162–180 in interleukin-1 receptor-associated kinase 1 (IRAK1), isoform 1 from *Mus musculus*. The peptide was synthesized and purified at Tufts University Medical School Core Facility (http://tucf.tufts.edu/home/peptide_synthesis), Boston, MA. All solutions were made with deionized distilled water (18.2 MΩ·cm). NMR and FTIR experiments were performed using glyphosate and peptide concentrations of 2 mM (1:1 molar ratio). The FTIR spectra of glyphosate sorbed on goethite have shown to be identical in 0.01, 0.1–0.2 M NaCl solutions (Yan and Jing, 2018). Therefore, $I \approx 0.01$ M was chosen to mimic a non-saline soil (i.e., EC = 0.7 mS/cm) using 10 mM KCl background electrolyte solutions. The experimental pH is fixed at 5, representing acidic soils of humid climates where the affinity of glyphosate for soil particles is high and where soils are rich in iron (hydr)oxides and organic matter (Chen et al., 2019; De Gerónimo and Aparicio, 2022; Ketterings et al., 2006; Pereira et al., 2019). Although many glyphosate studies at mineral surfaces have been conducted at near neutral and higher pH values, these pH values are not typical of agriculturally productive soils (Lin et al., 2012) and therefore do not broadly represent environmentally relevant conditions expected to influence glyphosate' behavior and fate. Reported acid dissociation constants for glyphosate are: pK_{a2} (carboxylic) = 2.23, pK_{a3} (phosphonic) = 5.46, and pK_{a4} (amine) = 10.14 (Chen et al., 2009; Li et al., 2013; Tribe et al., 2006), so that 72 % of glyphosate occurs as the monoanion [$^{-}OOCCH_2N^{+}H_2CH_2$-HPO_3^{-}] species at pH 5 and $I \approx 0.01$ M (Fig. S2). The chemical structure of glyphosate and the amino acid sequence of the peptide are presented in Fig. 1.

2.2. In-situ ATR-FTIR experiments

Attenuated total reflectance Fourier-transform infrared (ATR-FTIR) experiments were conducted with a Vertex 70 FTIR spectrometer (Bruker Corp. Billerica, MA). A Pike GladiATR accessory with a single bounce diamond IRE (internal reflection element) and flow through cell (Pike Technologies Madison, WI) were used for sampling. Spectra were collected from 4500 to 150 cm^{-1} with 4 cm^{-1} resolution and averaged over at least 104 scans. Post hoc treatment of spectra included atmospheric correction, Savitzky–Golay smoothing, and background correction to remove water vapor interference and instrumental drift. All spectral manipulations were performed using OPUS 7.2 software (Bruker Corp. Billerica, MA).

ATR-FTIR sorption experiments involved the acquisition of *in-situ* time-resolved spectra of glyphosate, the peptide, and glyphosate plus peptide (glyphosate + peptide, 1:1 molar ratio) solutions passed over a goethite film. Uniform evenly distributed goethite thin films were produced by drop casting a 4.8 μL aliquot of a goethite suspension (1.68 g L^{-1}) over the IRE and drying under N_2 flow. The thickness of the goethite film was optimized by conducting preliminary experiments (see Fig. S3 for details). Upon deposition and drying, a 10 mM KCl background electrolyte solution was passed over the film (rate ≈0.9 mL min^{-1}, which is equal to 0.013 m s^{-1}) to remove any loosely bound material and allow for re-hydration of the film. The stability of the goethite film is considered attained when no changes are observed in FTIR spectra collected during background solution flow. After goethite film stabilization, a background spectrum was collected and sorption experiments were initiated by exchanging the background solution with glyphosate, peptide, or glyphosate + peptide solutions. Sorption spectra were collected every 1.5 min until equilibration of surface species was observed. Bulk solution spectra of glyphosate (2 mM), peptide (2 mM), and glyphosate + peptide (2 mM each) were collected after drop casting a 100 μL aliquot over the IRE. The spectrum of the background electrolyte was subtracted from all spectra. Detailed ATR-FTIR protocols are described in previous publications (Azimzadeh and Martínez, 2024; Schmidt and Martínez, 2017; Schmidt and Martínez, 2018).

2.3. NMR experiments

All NMR experiments were acquired at 25 °C on a Varian INOVA 600 MHz spectrometer using a (H,C,N) z-axis gradient probe. Two-dimensional Rotating-Frame Overhauser Enhancement Spectroscopy (ROESY) (Bax and Davis, 1985; Bothner-By et al., 1984) spectra were

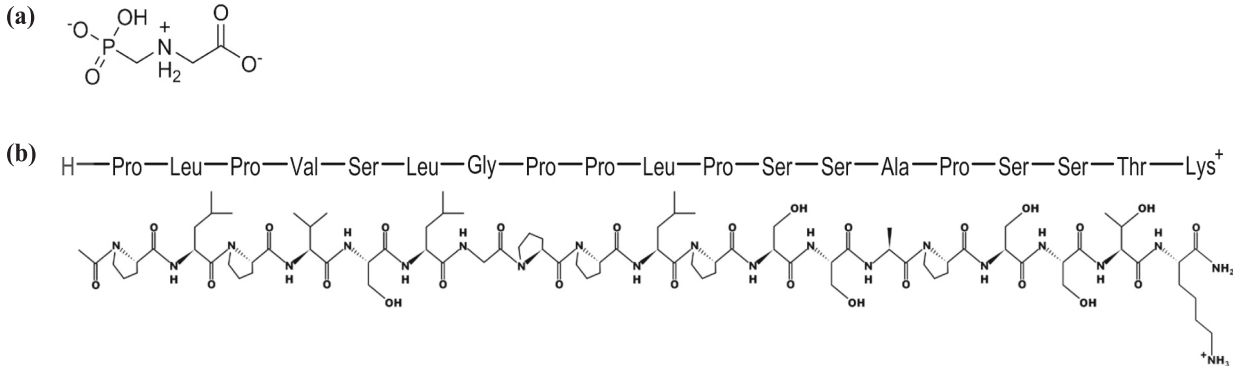

Fig. 1. Chemical structure of glyphosate (a) and amino acid sequence of the peptide (b). The peptide amino acid sequence in structural alphabet (SA) format is represented by PLPVSLGPPLPSSAPSSTK. Glyphosate, a zwitterion, occurs mostly (≈72 %) as the monoanion [$^{-}OOCCH_2N^{+}H_2CH_2$-HPO_3^{-}] species under experimental conditions (pH 5, $I \approx 10$ mM). The acetyl-amide blocked peptide, a model component of dissolved organic matter, contains 19 amino acids and has a molecular mass of ≈1831 g mol^{-1} (~1.8 kDa), a pI (isoelectric point) of 10.6, and a net charge of 1+ at pH 5.

acquired with 150 ms mixing time and spectral widths of 8.4 kHz in $t2$ (2048 complex data points) and in $t1$ (1024 complex data points). Two-dimensional Total Correlation Spectroscopy (TOCSY) (Bax and Davis, 1985) spectra were recorded with 70 ms mixing time and spectral widths of 8.4 or 10 kHz in $t2$ (2048 complex data points) and 8.4 kHz in $t1$ (1024 complex data points). All spectra were processed using nmrPipe (Delaglio et al., 1995) to perform polynomial water subtraction in the time domain, and phase-shifted sine bell apodization, a single zero-fill, Fourier transformation, zero and first-order phase correction, and linear baseline correction in each dimension.

2.4. Sorption kinetics

The kinetics of glyphosate, peptide, and glyphosate + peptide sorption experiments on goethite were assessed by fitting sorption kinetic models to the FTIR data. Peak heights of the glyphosate νP—O—Fe ($\approx$985 cm^{-1}) and of the peptide amide II ($\approx$1555 cm^{-1}) vibrations were plotted with time, and the pseudo-first order (PFO), pseudo-second order (PSO) and Elovich rate equations evaluated and fitted to obtain sorption kinetic model parameters (Aharoni and Tompkins, 1970; Ho, 2006; Plazinski et al., 2009). The νP—O—Fe vibration indicates inner-sphere sorption via the phosphonate group of glyphosate (Azimzadeh and Martínez, 2024; Barja and dos Santos Afonso, 2005; Sheals et al., 2002; Yan and Jing, 2018). The amide II band is used to monitor peptide sorption since this vibration is not as sensitive to structural changes or potential aggregation compared to amide I vibrations (Barth, 2007; Barth and Zscherp, 2002; Tamm and Tatulian, 1997). Our goal was to determine whether the extent and kinetics of the formation of inner-sphere P–O–Fe complexes between glyphosate and goethite were affected by the presence of the peptide; and conversely, to quantify the effect glyphosate might have on the extent of peptide sorption, mechanisms and sorption kinetics at the goethite surface. Description of sorption kinetic models tested is presented in the SI, and in previous work (Schmidt and Martínez, 2016).

2.5. Quantitative analyses of the peptide secondary structure

Deconvolution of the amide I band, which displays secondary structure sensitivity (Barth and Zscherp, 2002), was used to quantify changes in the peptide secondary structure during the sorption process and for the peptide in solution, both in the absence and presence of glyphosate. Deconvolution of the amide I band was performed with PeakFit package v.4.12 (Systat Software Inc., San Jose, CA). After post hoc treatment of the spectra, a linear baseline was fitted across the amide I band (1700–1600 cm^{-1}). To determine the position of overlapping components, the second derivative of IR spectra was employed in peak fitting. The second derivative treatment presents sharper bands and better resolution than the original spectra. Gaussian peaks were then added to the amide I band, with optimization of amplitude, peak position and width. To verify the reliability of identified components, the calculated components of a spectrum with fixed Gaussian parameters (e.g., at t_1) were applied to the next spectrum (e.g., at t_2), and vice versa. The results of this fitting method showed the identified components occurred at almost the same position ($\pm$5 cm^{-1}); however, the amplitude and width needed to be optimized. This iterative validation method was used across all kinetic data sets to minimize the impact of IR artifacts and overfitting. Fitting of the amide I band resulted in the identification of four structural component peaks. The goodness of fit R^2 factor for all fitted spectra was >0.999. Peak component positions and associated tentative secondary structure assignments are: A, extended β-strands (structured, strong interactions) from 1612 to 1622 cm^{-1}; B, random coils from 1632 to 1649 cm^{-1}; C, β-turns from 1652 to 1676 cm^{-1}, and D, extended β-strands (amorphous, weak interactions) from 1681 to 1702 cm^{-1} (Barth, 2007; Barth and Zscherp, 2002; Roach et al., 2005; Tamm and Tatulian, 1997). Peak component positions are inclusive of peptide and glyphosate + peptide, both in solution and sorbed on goethite.

The secondary structure of the peptide in solution was characterized from NMR chemical shifts of alpha protons (H^{α}) using the Chemical Shift Index (CSI) (Wishart et al., 1992). The difference ($\Delta\delta H^{\alpha}$) between the observed H^{α} chemical shift value and its corresponding random coil value for a given amino acid residue type provides a measure of secondary structure (Wishart et al., 1992). The CSI value is assigned +1 if $\Delta\delta H^{\alpha} > 0.1$ ppm, −1 if $\Delta\delta H^{\alpha} < -0.1$ ppm, and 0 if $-0.1 < \Delta\delta H^{\alpha} > +0.1$. Secondary structure was assigned based on the CSI values using the published protocol (Wishart et al., 1992).

3. Results and discussion

3.1. Solution spectra

Glyphosate in solution showed FTIR peaks typical of vibrational modes resulting from its carboxylate-amine envelope ($\nu_{as}(COO^-)$ + $\delta(NH_2^+)$, centered at $\approx$1615 cm^{-1}), and from carboxylate ($\nu_s(COO^-)$ at $\approx$1400 cm^{-1}), carbon-hydrogen/carbon-carbon ($\omega CH_2/\nu CC$ at $\approx$1325 cm^{-1}) and phosphonate ($\nu_{as}(PO_2)$ at $\approx$1186 cm^{-1}, $\nu_s(PO_2)$ at $\approx$1083 cm^{-1}, $\nu(PO_3)$ at $\approx$980 cm^{-1}) functional groups (Fig. 2a) (Sheals et al., 2003; Undabeytia et al., 2002; Yan and Jing, 2018). Similarly, vibrations typical of proteins appeared in the peptide solution spectrum that include the amide I (backbone ν(C═O) at $\approx$1675 cm^{-1} and backbone δ(NH) at $\approx$1625 cm^{-1}) and amide II (δ(NH) + ν(CN) at $\approx$1537 cm^{-1}) vibrational modes. Additional vibrations, not usually of high enough intensity to be observed in proteins, are clearly observed for the peptide. These vibrations arise from specific amino acids and their side chains (Figs. 2a, 1b, Table S1): δCH_2 at $\approx$1465 cm^{-1}; $\delta_{as}(CH_3)$ at $\approx$1440 cm^{-1}; δ(CH), τ CH_2, ω CH_2 at $\approx$1200 cm^{-1}; δCOH/νCO (serine, threonine) at $\approx$1138 cm^{-1}; and ν(CN) at $\approx$1050 cm^{-1} (Barth and Zscherp, 2002; Tamm and Tatulian, 1997).

Before conducting sorption studies with solutions containing glyphosate + peptide, we wanted to know whether glyphosate and the peptide interacted in solution. For this purpose, two dimensional (2D) homonuclear NMR (^1H—^1H ROESY, ^1H—^1H TOCSY) studies were conducted using a 1:1 glyphosate:peptide molar ratio in solution at pH 5 and in the presence of Ca^{2+} or K^+ electrolyte solutions. The ROESY experiment detects through-space interactions between H atoms that are within a 5 Å distance, while the TOCSY experiment shows through-bond connectivity between H atoms within 3 bonds of each other. As shown by comparison of the 2D ROESY and TOCSY spectra with and without glyphosate, no changes in the chemical environment of glyphosate or the peptide were observed (Fig. 2b–d), thus indicating that glyphosate and the peptide did not interact under the solution conditions tested. Notably, peaks corresponding to minor populations of *cis* prolyl peptide bonds are present at lower contour levels but also show no differences in chemical shift with and without glyphosate. FTIR results also indicated that glyphosate and the peptide did not interact in solution; in fact, the spectrum of glyphosate + peptide in solution contains all of the vibrations of individual glyphosate and peptide spectra, with no shifts in peak positions that would have suggested their interaction (Fig. 2a, Table S1). As reported in previous studies, the formation of biomolecule-rich supramolecular assemblies occur between relatively large DOM components (e.g., proteins, lipids, lignin, nucleic acids) (Schmidt and Martínez, 2018; Sutton and Sposito, 2005) while glyphosate seemed to interact with DOM components >5 kDa (e.g., hydrophilic fulvic acids and hydrophobic humic acids) (Li and Sato, 2017; Mazzei and Piccolo, 2012; Piccolo and Celano, 1994). Based on our spectroscopic evidence we however suggest solvation of the low molecular mass peptide (~1.8 kDa) precludes the formation of glyphosate-peptide complexes in solution. Although chemical modeling predicted the formation of a 1:1 glyphosate:pentaglycine (~0.30 kDa) soluble complex, these potential H-bond interactions have not been experimentally confirmed (Ahmed et al., 2018). Moreover, glyphosate interactions with small peptides are likely affected by the amino acid sequence and conformation of the peptide, including the potential for the formation of electrostatic interactions and H-bonds.

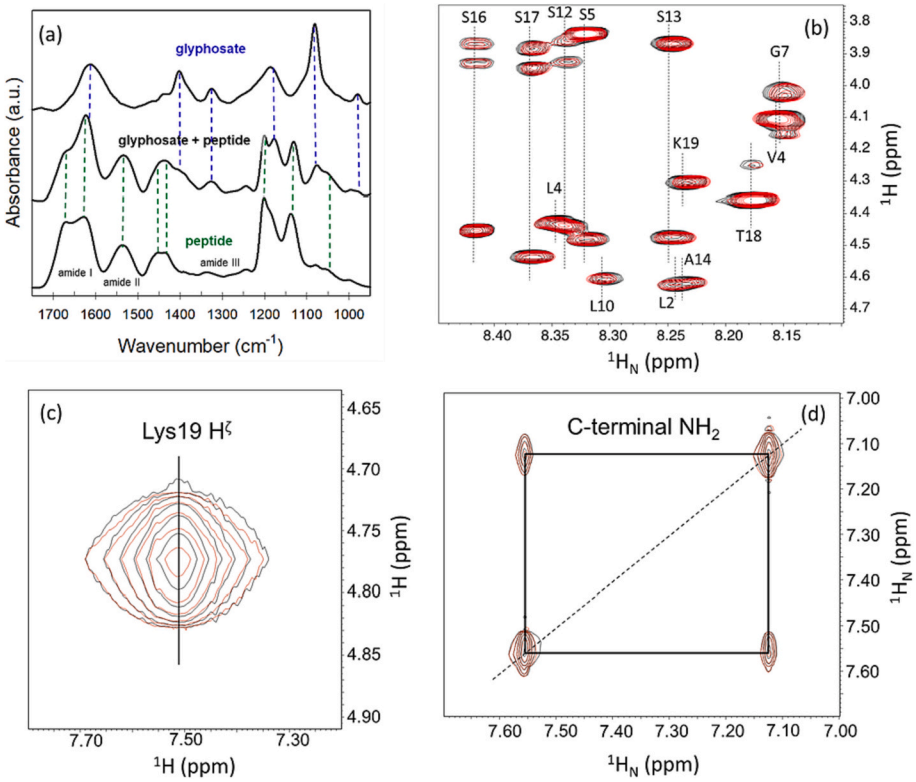

Fig. 2. Solution ATR-FTIR spectra (a) of glyphosate, glyphosate + peptide, and peptide. Vertical dashed lines in (a) indicate selected vibrations in the glyphosate + peptide spectrum that arise from glyphosate (indigo) and the peptide (green). Overlaid NMR TOCSY (b) and 2D-ROESY (c, d) of peptide (black) and peptide + glyphosate (red). (b) The H_N-H^{α} region of the TOCSY spectrum. Letter-number labels in (b) denote specific amino acids corresponding to the amino acid sequence (Fig. 1) in structural alphabet (SA) format: PLPVSLGPPLPSSAPSSTK. (c, d) Selected regions from the 2D-ROESY spectrum showing peaks arising from protons at or near the positive charged C-terminal end of the peptide.

3.2. Sorption spectra: competition and interactions

In-situ ATR-FTIR experiments were used to monitor the sorption of glyphosate, the peptide, and glyphosate + peptide onto goethite from solution in real time (Fig. 3). The progression of FTIR spectra of glyphosate sorbed on goethite, compared to that in solution, show differences that reveal the sorption mechanism (Fig. 3a). Glyphosate sorption on goethite shows the development of FTIR vibrations characteristic of an inner-sphere complex in which the phosphonate group of glyphosate binds to an Fe(III) center on the goethite surface (P–O–Fe bonds, within the ≈1075–989 cm^{-1} range) (Table S1) (Arroyave et al., 2016; Sheals et al., 2002). As reported in previous studies, a decrease in peak position of the carboxylate-amine band upon sorption ($\nu_{as}(COO^-)$ + $\delta(NH_2^+)$, centered at ≈1605 cm^{-1}) suggests the carboxylate and/or amine functionalities of glyphosate form outer-sphere complexes on goethite (Azimzadeh and Martínez, 2024; Yan and Jing, 2018), albeit inner-sphere complexes appear more prominent (Arroyave et al., 2016; Sheals et al., 2002). Glyphosate sorption had a negligible effect on goethite surface hydration (Fig. S4) that implies glyphosate displaced little water from the goethite surface upon sorption. In contrast, the adsorption of peptide onto goethite appears to be coupled to water displacement at the interface, as suggested by a pronounced decrease in vibrational bands associated with goethite' interfacial water (Fig. S4).

Peptide sorption onto goethite is highlighted by FTIR spectra through increasing signals of amide II (backbone in-plane δ(NH) and ν(CN), ≈1580–1500 cm^{-1}), amide III (in-phase backbone δ(NH) and ν(CN), ≈1400–1225 cm^{-1}) and ν(CN) (≈1072 cm^{-1}) bands with time (Fig. 3c, Table S1) (Barth and Zscherp, 2002; Roach et al., 2005; Tamm and Tatulian, 1997). Compared to peptide in solution, sorbed peptide C—H (≈1200 cm^{-1}) and δCOH/νCO (≈1150 cm^{-1}) vibrations decreased in relative intensity, but while δCOH/νCO vibrations shifted to higher frequency (≈1138 to ≈1150 cm^{-1}), C—H vibrations did not. Although the intensity and frequency of the $\delta(CH_2)_{proline}$ vibration (≈1465 cm^{-1}) did not seem to change upon peptide sorption, the $\delta_{as}(CH_3)$ vibration (≈1440 cm^{-1}) all but disappeared. These changes to the spectra suggest the peptide interacted with the goethite surface through functional groups present in its backbone, as well as through the side chains of serine and threonine (COH functionalities) (Fig. 1b) via H-bonds. In particular, CH_3 functional groups of side chains of leucine and valine appeared to point away from the hydrophilic goethite surface upon sorption. A decrease in signal intensity and increase broadening of the amide I band is however observed with sorption time (Fig. 3c). Since bandwidth is a measure of conformational freedom (i.e., flexible structures have broader bands compared to rigid structures) (Barth and Zscherp, 2002), broadening of the amide I band suggests changes in peptide conformation occurred during sorption (Yang et al., 2022; Yang et al., 2021). As discussed below, deconvolution of the amide I band revealed conformational changes to the peptide upon sorption onto goethite did occur. In contrast to the glyphosate-goethite interaction, peptide sorption on goethite was coupled to a decrease in surface hydration (decreased intensity of the ν(H—O—H) vibration at ≈3186 cm^{-1}; Fig. S4) which likely results from a higher proportion of the peptide being probed, instead of water, relative to background spectrum. Sorption can then be understood to result from retention of a weakly or non-polar molecule (i.e., the peptide) at a hydrophilic surface (i.e., goethite) where surface hydration energy (surface-water interaction) is insufficient to counter the water-water bonding energy that forces the molecules out of solution. This is known as the hydrophobic effect - the tendency of water to exclude non-polar molecules from solution - and it is considered to be entropy-driven (Adamson and Gast, 1997). Entropic contributions from surface dehydration have been observed in peptide and protein sorption studies that further suggest the

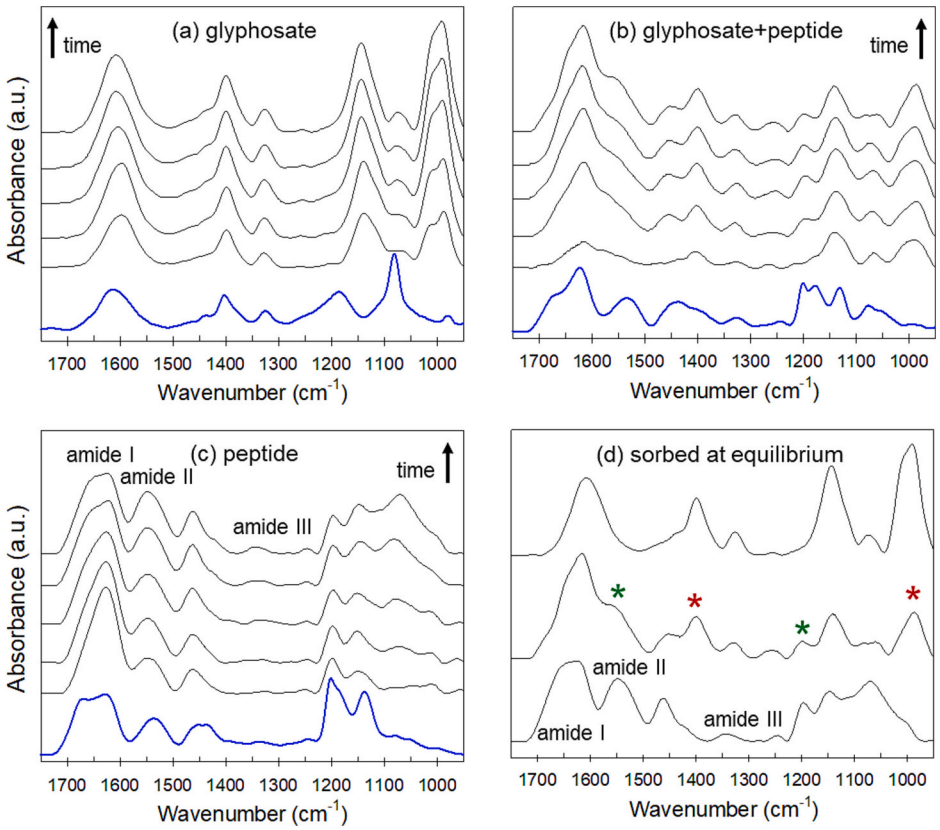

Fig. 3. ATR-FTIR spectra from sorption experiments at the goethite interface representing the time evolution (1.5 to 27 min) of spectral features for (a) glyphosate, (b) glyphosate + peptide and (c) peptide, with corresponding solution spectra (blue lines). (d) Sorption equilibrium spectra of glyphosate (top), glyphosate + peptide (middle), and peptide (bottom). Asterisks in (d) indicate selected vibrations in the glyphosate + peptide spectrum that arise from glyphosate (red) and the peptide (green).

peptide interacts with the goethite surface through electrostatic and H-bond interactions (Schmidt and Martínez, 2016; Touzeau et al., 2021; Yang et al., 2022) while at the same time been excluded from bulk water by the hydrophobic effect. Given the lack of interaction between glyphosate and the peptide in solution, the glyphosate + peptide sorption ATR-FTIR spectra can be interpreted as the result of competition between glyphosate and the peptide for the goethite surface. Sorption experiments with solutions containing glyphosate + peptide showed spectral features that indicate both glyphosate (e.g., P–O–Fe at ≈985 cm^{-1}, $\nu_s(COO^-)$ at ≈1400 cm^{-1}) and the peptide (e.g., amide II at ≈1555 cm^{-1}, C—H at ≈1200 cm^{-1}) sorbed onto goethite (Fig. 3d, Table S1) and that this was a dynamic process (Fig. 3b). Shifts in peak position as well as changes in peak intensity and bandwidth were however apparent and suggest interfacial species formed from glyphosate + peptide solutions differ from those of solutions containing either glyphosate or the peptide. Narrowing of the amide I band (≈1700–1600 cm^{-1}) of sorbed glyphosate + peptide at equilibrium compared to sorbed peptide at equilibrium (Fig. 3d) and solution glyphosate + peptide spectrum (Fig. 3b) indicated the presence of glyphosate at the goethite surface induced changes to the peptide conformation or structure (Barth and Zscherp, 2002). Broadening and a shift of the amide II band (backbone in-plane δ(NH) and ν(CN)) to higher frequency (Fig. 3b) suggested the formation of H-bonds between the peptide and the goethite surface; still, the observed decrease in intensity suggested glyphosate limits their interaction (Fig. 3d) (Barth and Zscherp, 2002; Colthup, 2012). In glyphosate + peptide-goethite, the C—H vibration of sorbed peptide (≈1200 cm^{-1}) was initially absent but emerged during sorption (Fig. 3b). In contrast to peptide-goethite, the $\delta(CH_2)_{proline}$ vibration (≈1465 cm^{-1}) of the peptide occurred at a lower frequency upon glyphosate + peptide sorption (Table S1) whereas the $\delta_{as}(CH_3)$ vibration (≈1440 cm^{-1}) was present in glyphosate + peptide-goethite. It is likely the peptide in glyphosate + peptide also formed H-bonds with goethite through the side chains of serine and threonine (δCOH/νCO at ≈1150 cm^{-1}), however, this is difficult to demonstrate due to overlap with the glyphosate-goethite ν(P═O) vibration (Fig. 3d). Although the peptide in glyphosate + peptide-goethite seems to interact with the surface in ways similar to those in peptide-goethite (i.e., H-bonds with backbone and side chains), we suggest sorption of additional peptide conformers in glyphosate + peptide-goethite account for the observed differences in spectral features (e.g., amide I and $\delta_{as}(CH_3)$ of leucine and valine). As with the peptide, sorption of glyphosate + peptide appears to displace water from goethite (Fig. S4), further suggesting the formation of H-bonds at the interface (Touzeau et al., 2021; Yang et al., 2022). Moreover, comparison of the ν(P—O) region (≈1175–950 cm^{-1}) of glyphosate and glyphosate + peptide indicated shifts in peak positions and changes to peak intensities and bandwidths occurred in the presence of the peptide (Fig. 3a, b, d; Table S1). Comparison of relative ratios of peaks at ≈1082 cm^{-1} ($\nu(P—O—Fe)_{M\text{-}H}$ + $\nu(PO_2)_{OS}$) and ≈1016 cm^{-1} ($\nu_{as}(P—O—Fe)_{B/M}$) indicates a preference for the formation of mononuclear monodentate (M) and outer-sphere (OS) glyphosate complexes in glyphosate + peptide-goethite over binuclear bidentate (B) or mononuclear monodentate in glyphosate-goethite (Fig. 3d) (Azimzadeh and Martínez, 2024; Yan and Jing, 2018). This analysis suggests the phosphonate group of glyphosate tends to form outer-sphere complexes with goethite when the peptide is present at the surface. It is therefore possible that the peptide modulates glyphosate sorption mechanism onto goethite by competing for surface sorption sites and that competition is determined by the hydrophobic effect (Adamson and Gast, 1997) and by steric shielding effects where the charged groups on glyphosate are seemingly weakened or spatially shielded by the less

charged sorbed peptide (Day et al., 1997). Once at the goethite surface, glyphosate and the peptide do not appear to interact to any significant degree.

3.3. Sorption kinetics

The sorption kinetics of glyphosate and the peptide onto goethite were followed using the absorbance of the inner-sphere νP—O—Fe (≈985 cm^{-1}) vibration of glyphosate and that of the amide II (≈1555 cm^{-1}) vibration of the peptide (Fig. 4). These vibrational modes were selected since they are distinct to glyphosate and the peptide, and their peak heights can be easily quantified. Three sorption kinetic models were tested: pseudo-first order (PFO), pseudo-second order (PSO) and Elovich. Description of sorption kinetic models, linearized sorption kinetic rate plots (Fig. S5) and resulting kinetic parameters (Table S2) can be found in the supplementary information. The sorption rate equations tested are typically used to describe surface controlled sorption kinetics (i.e. sorption rates limited by interfacial energetic barriers) and consider the sorption capacities of solids (Plazinski et al., 2009). Surface-related energetic restrictions have been suggested as the primary limitations on sorption rates of proteins (Schmidt and Martínez, 2016). Under experimental conditions, sorption kinetics from glyphosate, peptide, and glyphosate + peptide solutions were well described by the pseudo-second-order sorption kinetic model (high R^2, low RMSE, visual inspection) and reached pseudo-equilibrium conditions within 5–20 min (Figs. 4, S5). The PSO model represents a kinetic order of two with respect to the number of available sorption sites, for example, protonated and deprotonated hydroxyls at the hydrophilic goethite surface (pH_{pzc} = 8.4 ± 0.2) (Ho, 2006; Plazinski et al., 2009). We can in principle compare the effect of the peptide on glyphosate inner-sphere sorption kinetics since the νP—O—Fe vibration only arises upon glyphosate sorption; likewise, the amide II band only arises upon sorption of the peptide (Plazinski et al., 2009). Note however the rate constants determined represent *observed* rate constants under the experimental conditions tested.

As clearly illustrated in Fig. 4a, the peptide hinders the formation of inner-sphere νP-O-Fe bonds between glyphosate and goethite, with ≈80 % reduction at equilibrium (Fig. S6). The peptide therefore seems to block surface reaction sites that would otherwise be available to glyphosate even though the strength of glyphosate-goethite (inner-sphere) and peptide-goethite (outer-sphere) sorption mechanisms are presumed to differ. In addition to steric shielding effects (Day et al., 1997), energetic considerations can explain the reduction in glyphosate inner-sphere sorption since the molecule with the lower activation energy for sorption (from ΔH, enthalpy, considerations; e.g., H-bonding of the peptide) is expected to preferentially sorb (Aharoni and Tompkins, 1970). Furthermore, the hydrophobic effect increases the entropy (ΔS) of the system upon peptide sorption while entropy contributions to glyphosate sorption are likely negligible (Adamson and Gast, 1997). The observed PSO rate constant (k_2) for the formation of νP—O—Fe bonds between glyphosate and goethite was higher in the presence of the peptide (k_2 = 807.9 ± 162.9 $a.u.^{-1}$ min^{-1}) compared to that in its absence (k_2 = 296.4 ± 21.4 $a.u.^{-1}$ min^{-1}). This increase in observed rate constant likely results from reduced sorption of glyphosate from glyphosate + peptide solutions ($q_e = 2.3 \times 10^{-3}$ (a.u.) for glyphosate and 4×10^{-4} (a.u.) for glyphosate + peptide) that reached equilibrium after 5 min (Plazinski et al., 2009). Similarly, the presence of glyphosate reduced the extent of peptide interactions with the surface, albeit to a lesser degree (≈30 % reduction at equilibrium) (Figs. 4b, S6). Glyphosate, however, had a smaller and opposite effect on the observed sorption rate constants of the amide II band of the peptide, with k_2 = 887.9 ± 178.9 $a.u.^{-1}$ min^{-1} for glyphosate + peptide and k_2 = 983.7 ± 133.3 $a.u.^{-1}$ min^{-1} for the peptide. It has long been interpreted that lower rate constants in binary systems express the condition of simultaneous sorption where each molecule competes for the available sorption sites (Aharoni and Tompkins, 1970). Since the k_2 value for νP—O—Fe (296.4 $a.u.^{-1}$ min^{-1}) is about three times smaller than that for amide II (983.7 $a.u.^{-1}$ min^{-1}) in single systems, it appears differences in interfacial energetic barriers for the formation of glyphosate-goethite and peptide-goethite complexes dictate sorption preference (Aharoni and Tompkins, 1970; Plazinski et al., 2009). Plotting of [glyphosate νP—O—Fe/peptide amide II] peak height ratios with time in glyphosate + peptide experiments (Fig. S6) revealed a decrease from ≈1.75 at 1.5 min to ≈0.75 at ≥3 min further highlighting a distinction in sorption behavior where the peptide outcompetes glyphosate for reaction sites at the goethite surface. A previous co-sorption study with glyphosate and aquatic DOM also found an increase in DOC:glyphosate-C ratio (≈17) upon sorption on goethite compared to the same ratio in solution (≈11.4) (Day et al., 1997). These authors used these parameters to justify surface competition and shielding models and to conclude that DOM sorption affinity for goethite was much greater than that of glyphosate. Furthermore, they found the DOM adsorbed onto goethite consisted almost entirely of the hydrophobic fraction, with the hydrophilic fraction remaining in solution. Their results agree with our findings that the goethite surface becomes more hydrophobic upon peptide sorption, and that increased hydrophobicity lowers glyphosate sorption. Evidence for increase in surface hydrophobicity upon peptide sorption are CH_3 vibrations that point away from the surface and entropic contributions from surface dehydration.

3.4. Conformational changes to the secondary structure of the peptide

Deconvolution of the amide I FTIR band was used to quantify changes in the peptide secondary structure in solution and during sorption, both in the absence and presence of glyphosate. Results of these analyses are shown in Fig. 5 while examples from deconvolution of spectra are presented in Fig. S7 and position of peak components with tentative secondary structure assignments are detailed in Tables S3 and

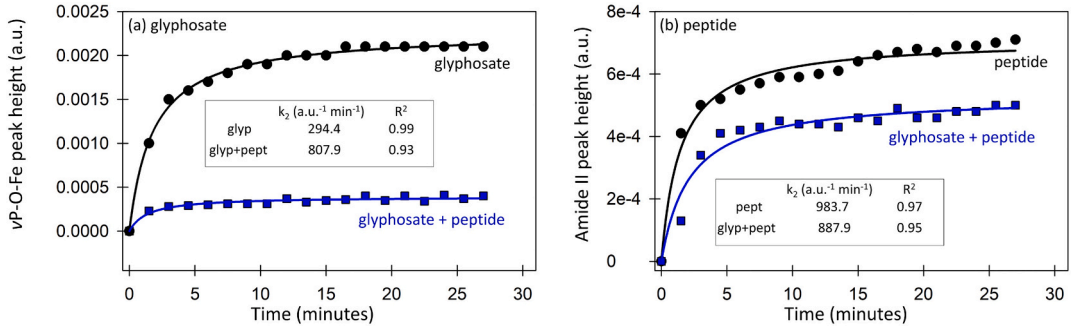

Fig. 4. Sorption kinetic plots for (a) glyphosate νP—O—Fe (at ≈985 cm^{-1}) and (b) peptide amide II (at ≈1555 cm^{-1}) vibrational modes. Plots represent experiments with glyphosate (glyp) and peptide (pept) individually (black circles) and in combination (glyp + pept, blue squares). Pseudo-second order (PSO) kinetic models for each series are depicted by lines of corresponding color.

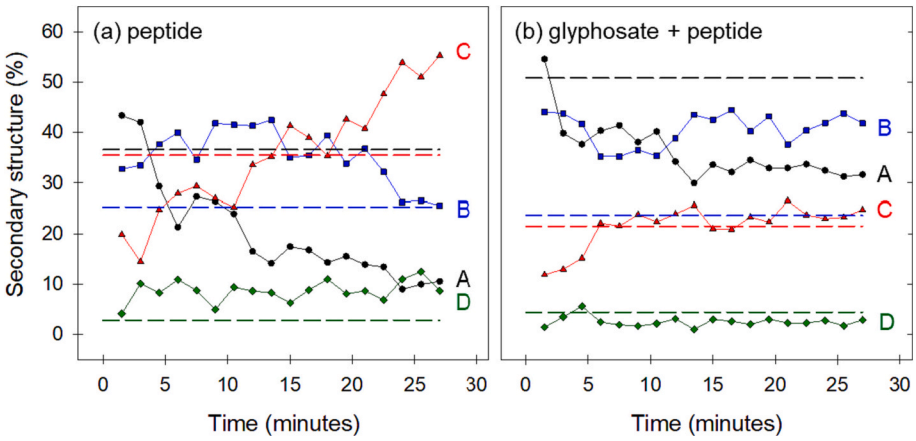

Fig. 5. Amide I curve fitting results for (a) peptide and (b) glyphosate + peptide spectra throughout the sorption process (symbols with connecting lines) and in solution (horizontal dashed lines of corresponding color). Peptide secondary structure assignments are: A, structured β-strands; B, random coils; C, β-turns; D, amorphous β-strands.

S4. Small peptides are often highly flexible, and the amide bands associated with different secondary structural elements in peptides can therefore show deviations from those observed with large water-soluble folded proteins (Goormaghtigh et al., 2006). Fundamental understanding of peptide and protein conformations (Nelson and Cox, 2021; Pal, 2019; Stryer et al., 2019) as well as previous publications (Barth, 2007; Roach et al., 2005; Tamm and Tatulian, 1997) informed our secondary structural assignments. Extended β-strands represent a section of the peptide chain (typically 3–10 amino acids long) with backbone in an extended conformation. β-strands refer to conformations that result from intramolecular interactions within the peptide chain as well as from processes during which peptide molecules associate into larger species consisting of multiple peptide chains (intermolecular interactions) (Zapadka et al., 2017). Peptide chains can interact to form amorphous or structured β-strands. The formation of β-strands (amorphous and structured) might occur in solution or might be induced by a solid surface. Hydrogen bonds and hydrophobic interactions may promote the formation of structured β-strands thus increasing their stability and lowering their energy. We consider structured β-strands are reflected by peak components at low frequency whereas amorphous β-strands occur at high frequency (Zapadka et al., 2017). Random coils are polymer conformations where the amino acid residues are free to randomly sample many conformations (i.e., an unstructured peptide chain), and while they do not represent one precise shape, in the presence of specific, stabilizing interactions, the polymer can prefer one conformation over all others (Goormaghtigh et al., 2006; Zapadka et al., 2017). In contrast, β-turns afford a special relation between structure and residue type, with five amino acid residues (aspartic acid, glycine, proline, asparagine, serine) seen more often than all others in β-turns (Pal, 2019; Stryer et al., 2019). In β-turns, the C═O of one amino acid is H-bonded to the N—H group of an amino acid three residues away. Among the 19 amino acid residues present in the peptide, 12 of them (6 proline, 5 serine, 1 glycine) are prone to form β-turns (Fig. 1).

Based on amide I FTIR analyses, the secondary structure of peptide molecules in solution was determined to include structured β-strands (~37 %), random coils (~25 %), β-turns (~35 %), and amorphous β-strands (~3 %) (Fig. 5a). These results are consistent with model outputs of the predicted secondary structure of the peptide chain in solution using PEP-FOLD3 (Lamiable et al., 2016), where β-turns and random coil conformations are apparent (Fig. S8). However, deconvolution of the amide I band also indicates the peptide forms β-strands in aqueous solution suggesting the solution does not exclusively contain peptide monomers (Yang et al., 2022). The presence of glyphosate in solution resulted in an increase in structured β-strands (~51 %) and a decrease in β-turns (~21 %) with no substantial differences in the structural content of random coils (~24 %) and amorphous β-strands (~4 %) (Fig. 5b). These changes suggest the presence of glyphosate promoted the formation of intermolecular interactions among peptide chains that increased the proportion of structured β-strands while reducing the peptide intramolecular interactions and thus the proportion of β-turn structures (Yang et al., 2022). These changes involve the formation and rupture of H-bonds.

Consistent with FTIR results, structural analysis of the peptide using ^{1}H NMR chemical shifts of the α-CH protons identified extended β-strand, random coil, and β-turn structural components (Fig. 6). The peptide sample without glyphosate was used to assign ^{1}H resonances and to characterize the secondary structure of the major conformation of this peptide. Since no significant peak changes were observed after addition of glyphosate to the peptide, this characterization also applies to the peptide in the presence of glyphosate. Based solely on these $\Delta\delta H^{\alpha}$ values, residues 4–10 are classified as β-strand. A β-turn involving the N-terminal acetyl group and residues 1–3 (acetyl-PLP) appears to be present, based on the −1,+1 pattern (Wishart et al., 1992). Notably, a β-turn is defined by the phi-psi torsion angles of the central two residues only, without restriction on the phi-psi values of the flanking residues. The remaining residues (11–19) are classified as random coil. The random coil designation can also contain transient β-turn conformations. Since the PolyProline type II helix (PPII) is difficult to distinguish from the extended β-strand by NMR, it is likely that parts of the N-terminal half of this peptide adopt the PPII conformation. Notably, the two methyl groups of Leu6 show distinct chemical environments as do the two H^{α}s of Gly7, indicating a more stable structure in this region. One observed difference between the peptide and peptide + glyphosate is an overall ~20 % reduction in peak intensities when glyphosate is present. This loss of signal could result from formation of large aggregates with rotational rates too slow for detection by NMR, and would be consistent with the FTIR findings if formation of these aggregates involved conversion of random coil to extended β-strand.

Results also indicated peptide-goethite surface interactions modified the secondary structure of the peptide, compared to that of the peptide in solution (Fig. 5a). Throughout the sorption process, reduced contributions from structured β-strands (~44 to ~10 %) and random coils (~33 to ~25 %) were observed while the contribution from amorphous β-strands remained relatively constant (~5–10 %). Accompanying these changes was a continuous increase in β-turn content from ~20 to ~56 %. Although peptide-goethite sorption reached a pseudo-equilibrium condition within ~15 min (Fig. 4b), the sorbed peptide continued to change towards a more compact structure with more β-turns (Figs. 3c, 5a, S6). At experiment's end, a net decrease in β-strands (~20 %) and an increase in β-turns (~56 %), compared to peptide in solution (~40 %

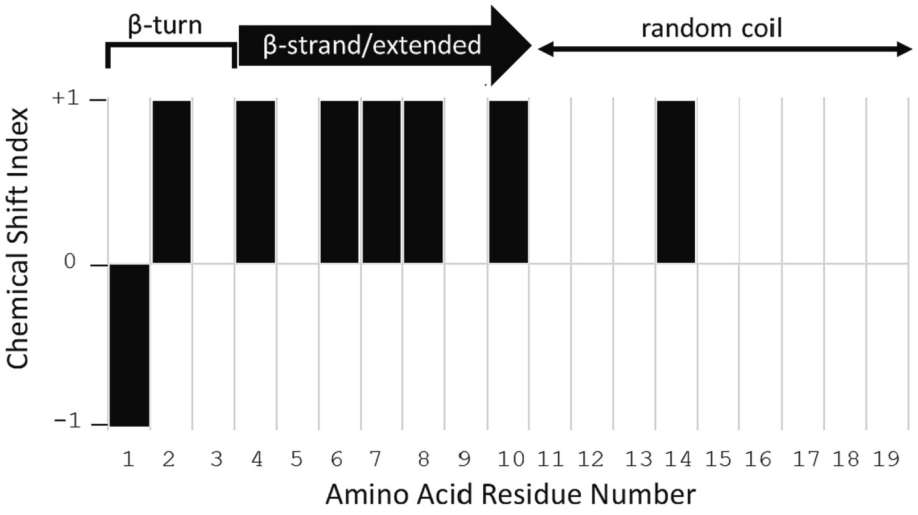

Fig. 6. Peptide secondary structure from NMR Chemical Shift Index. The location and identity of secondary structure are shown above a plot of the Chemical Shift Index value for Hα protons versus amino acid sequence.

β-strands, ~35 % β-turns), suggest a surface-induced rupture of intermolecular H-bonds among peptide chains and a preference for sorption of more compact peptide conformers that simultaneously promote H-bond formation between the peptide and the goethite surface. Our structural analyses are indeed in agreement with sorption mechanisms where time-resolved ATR-FTIR spectra (Fig. 3) indicate the formation of H-bonds between C–OH functionalities of side chains of serine and threonine and goethite (Liu et al., 2022). Observed conformations are consistent with the most frequently found conformations (i.e., β-turn and random coil) reported for a 17-residue (Yang et al., 2022) and for a 5-residue (Touzeau et al., 2021) peptide sorbed onto hydrophilic surfaces. In addition, changes to H-bond networks have been observed where intramolecular peptide interactions that induce a more compact conformation are favored (Touzeau et al., 2021; Yang et al., 2022; Yang et al., 2021).

Competitive sorption studies (glyphosate + peptide) at the goethite interface revealed further changes to the peptide secondary structure occurred during sorption, which stabilized after ≈15 min (Fig. 5b). At experiment's end, compared to glyphosate + peptide in solution, the content of β-turns (~24 %) and amorphous β-strands (~2.5 %) was similar, while the content of structured β-strands was lower (32 %) and that of random coils was higher (~40 %) in glyphosate + peptide-goethite. As with peptide-goethite interactions, the goethite surface in glyphosate + peptide promoted the partial disruption of intermolecular H-bonds among peptide chains in favor of H-bond formation with the surface. Sorbed peptide conformations however differed in the presence and absence of glyphosate, with preference for random coils and structured β-strands in glyphosate + peptide-goethite and for β-turns in peptide-goethite (Fig. 5). Although glyphosate had a small effect on the position of peak components for peptide in solution and sorbed onto goethite (Table S4), corresponding component peak positions decreased considerably in sorption spectra compared to solution spectra thus indicating the goethite surface had a greater effect on the secondary structure of the peptide. A lower frequency of component peak position indicates lower energy, which can be interpreted as higher stability through the formation of H-bonds with the goethite surface. Overall, the shared effect of glyphosate (i.e., in solution and at the surface) was a reduction in β-turn structures accompanied by an increase in structured β-strands whereas that of the goethite surface was a reduction in structured β-strands (Fig. 5). The combined effect of glyphosate and goethite on the native peptide solution conformation was the formation and sorption of random coils that enhance the fraction of peptide molecules that undergo molecular spreading over the surface. We posit adoption of a random coil conformation permits the displacement of water molecules from the interface that increases the entropy of the system with a concomitant decrease in free energy (Palafox-Hernandez et al., 2014; Walsh and Knecht, 2017).

4. Conclusions

Organic molecules can be retained by a mineral surface through inner-sphere (e.g., ligand exchange) and outer-sphere (e.g., H-bonding, electrostatic) interactions, a situation that can be predicted for most metal oxide minerals such as goethite. Glyphosate and peptide sorption behavior (extent, kinetics, interfacial species) in binary systems (glyphosate + peptide) differ from that in single systems (Fig. 7), a result of competition for goethite sorption sites. Changes in goethite' surface charge and abundance of active sites during the adsorption process, as well as the hydrophobic effect that promotes peptide sorption, most likely alter glyphosate and peptide sorption dynamics. Co-sorbed peptide is expected to lower goethite' positive surface charge (Azimzadeh and Martínez, 2024), thus promoting the formation of glyphosate outer-sphere and mononuclear inner-sphere species while reducing the extent of glyphosate sorption (Fig. 7). We also observe that upon sorption, both in the presence or absence of glyphosate, the peptide adopts conformations that seem to facilitate contact with the goethite surface via H-bonds. It is perhaps this ability to change conformation that provides the peptide a competitive advantage over glyphosate for sorption at the goethite surface. Furthermore, sorption of peptide conformers that cover more of the surface seems to limit glyphosate sorption.

Overall, the presence of the peptide weakened glyphosate-goethite interactions (outer-sphere favored, inner-sphere hindered) whereas the presence of glyphosate limited peptide-goethite sorption. The results thus highlight potential effects the addition of organic contaminants, such as glyphosate, might have for the availability of nutrients (e.g., nitrogen) since peptides (and proteins) are a substantial N source in soils, but only a fraction of the sorbed biopolymer is bioavailable. In a sense, glyphosate' behavior is similar to the behavior of root exudates (low-molecular-weight organics) where their release may prevent or decrease peptide sorption, or may enhance the solubility and bioavailability of N-containing biomolecules from soil particle surfaces. The experimental results have significant implications regarding the mobility and transport of glyphosate in terrestrial environments. Experimental results presented here indicate biomolecules present in the soil aqueous phase (i.e., DOM components such as peptides) have the capacity to outcompete glyphosate for retention at mineral surfaces.

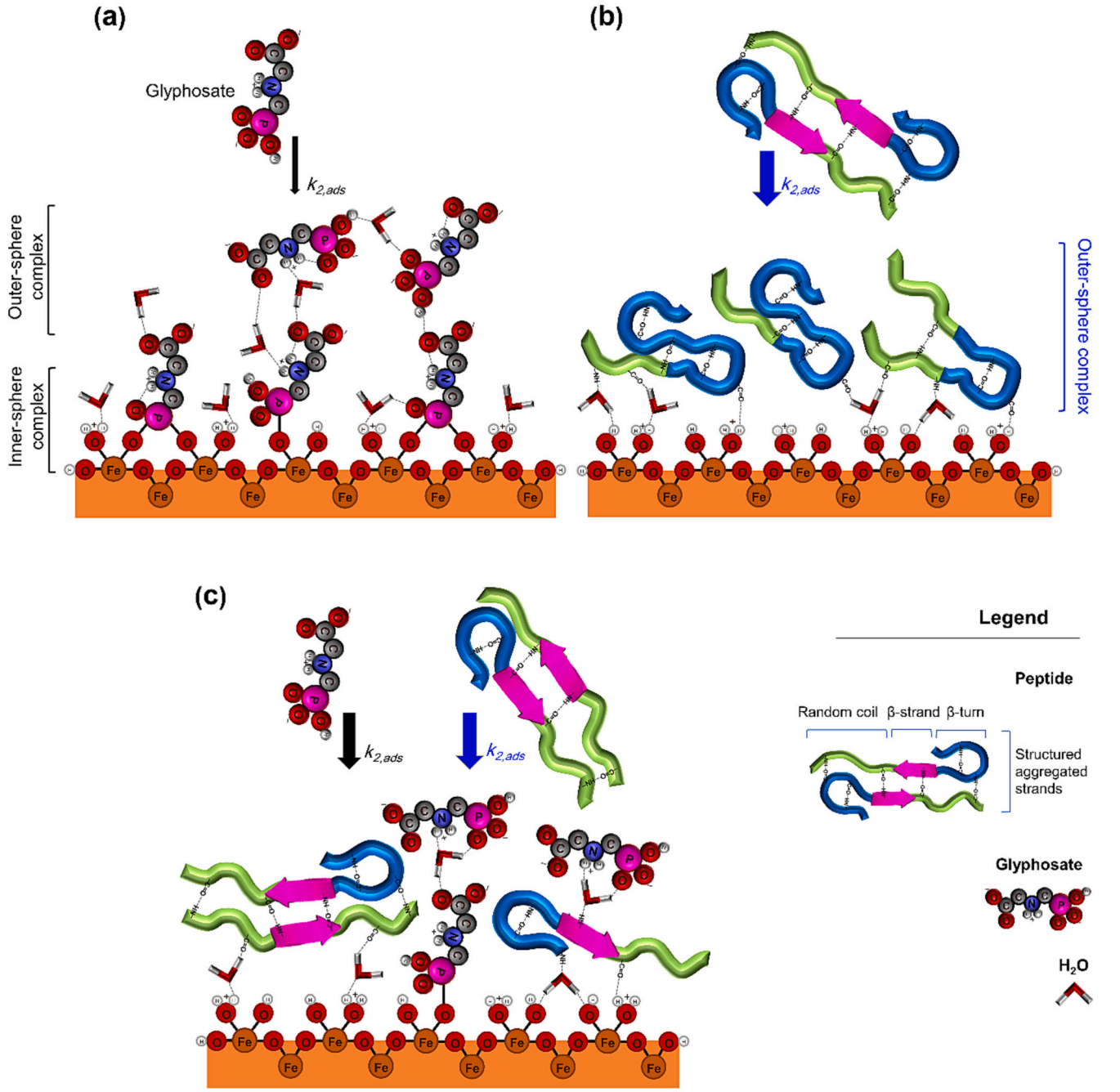

Fig. 7. A conceptual schematic illustrating adsorption of (a) glyphosate and (b) peptide in single systems, and (c) co-sorption of glyphosate and peptide in binary systems at the water/goethite interface at pH 5. In peptide molecules: blue, purple and green segments represent β-turn, β-strand and random coil, respectively. Black and blue arrows represent adsorption of glyphosate and peptide molecules through P—O and amide II moieties, respectively. The width of the arrows indicates the adsorption rate for their respective interfacial IR bands.

Sorption and accumulation of glyphosate in soils should therefore be considered a transient and reversible process where reactions with soil components create a reservoir with slow-release capability, which leads to the frequent and widespread detection of glyphosate and is a route to surface and groundwater contamination.

CRediT authorship contribution statement

Behrooz Azimzadeh: Conceptualization, Formal analysis, Investigation, Visualization, Writing – original draft, Writing – review & editing. **Linda K. Nicholson:** Conceptualization, Formal analysis, Investigation, Visualization, Writing – original draft, Writing – review & editing. **Carmen Enid Martínez:** Conceptualization, Formal analysis, Funding acquisition, Project administration, Resources, Supervision, Visualization, Writing – original draft, Writing – review & editing.

Declaration of competing interest

The authors declare that they have no known competing financial interests or personal relationships that could have appeared to influence the work reported in this paper.

Data availability

Data will be made available on request.

Acknowledgments

Funding for this work was provided by the National Science Foundation (Award number CHE-2003505) and by the USDA National Institute of Food and Agriculture, Hatch project (accession no. 1020955). Graduate financial support for B.A. was provided by the Agriculture and Food Research Initiative (AFRI, grant no. 2016-67019-25265/project accession no. 1009565) from the USDA National Institute of Food and Agriculture and by the College of Agriculture and Life Sciences at Cornell University. This work made use of the Cornell Center for Materials Research Shared Facilities supported by the National Science Foundation MRSEC program under Award Number DMR-1719875.

Appendix A. Supplementary data

Description of sorption kinetic models, 4 tables, 9 figures, and references. Supplementary data to this article can be found online at https://doi.org/10.1016/j.scitotenv.2023.169264.

References

Adamson, A., Gast, A., 1997. Physical Chemistry of Surfaces. A Wiley-Interscience Publication.
Aharoni, C., Tompkins, F.C., 1970. Kinetics of adsorption and desorption and the Elovich equation. In: Eley, D.D., Pines, H., Weisz, P.B. (Eds.), Advances in Catalysis, 21. Academic Press, pp. 1–49.
Ahmed, A., Chaker, Y., Belarbi, E.H., Abbas, O., Chotard, J.N., Abassi, H.B., et al., 2018. XRD and ATR/FTIR investigations of various montmorillonite clays modified by monocationic and dicationic imidazolium ionic liquids. J. Mol. Struct. 1173, 653–664.
Albers, C.N., Banta, G.T., Hansen, P.E., Jacobsen, O.S., 2009. The influence of organic matter on sorption and fate of glyphosate in soil–comparing different soils and humic substances. Environ. Pollut. 157, 2865–2870.
Aparicio, V.C., De Gerónimo, E., Marino, D., Primost, J., Carriquiriborde, P., Costa, J.L., 2013. Environmental fate of glyphosate and aminomethylphosphonic acid in surface waters and soil of agricultural basins. Chemosphere 93, 1866–1873.
Arroyave, J.M., Waiman, C.C., Zanini, G.P., Avena, M.J., 2016. Effect of humic acid on the adsorption/desorption behavior of glyphosate on goethite. Isotherms and kinetics. Chemosphere 145, 34–41.
Avigliano, E., Schenone, N.F., 2015. Human health risk assessment and environmental distribution of trace elements, glyphosate, fecal coliform and total coliform in Atlantic Rainforest mountain rivers (South America). Microchem. J. 122, 149–158.
Azimzadeh, B., Martínez, C.E., 2024. Unraveling the role of polysaccharide-goethite associations on glyphosate' adsorption–desorption dynamics and binding mechanisms. J. Colloid Interface Sci. 653, 1283–1292.
Barja, B., dos Santos Afonso, M., 2005. Aminomethylphosphonic acid and glyphosate adsorption onto goethite: a comparative study. Environ. Sci. Technol. 39, 585–592.
Barth, A., 2007. Infrared spectroscopy of proteins. Biochim. Biophys. Acta (BBA) Bioenergetics 1767, 1073–1101.
Barth, A., Zscherp, C., 2002. What vibrations tell about proteins. Q. Rev. Biophys. 35, 369–430.
Battaglin, W.A., Kolpin, D.W., Scribner, E.A., Kuivila, K.M., Sandstrom, M.W., 2005. Glyphosate, other herbicides, and transformation products in midwestern streams, 20021. JAWRA J. Am. Water Resour. Assoc. 41, 323–332.
Battaglin, W.A., Meyer, M., Kuivila, K., Dietze, J., 2014. Glyphosate and its degradation product AMPA occur frequently and widely in US soils, surface water, groundwater, and precipitation. JAWRA J. Am. Water Resour. Assoc. 50, 275–290.
Bax, A., Davis, D.G., 1985. Practical aspects of two-dimensional transverse NOE spectroscopy. J. Magn. Reson. (1969) (63), 207–213.
Bothner-By, A.A., Stephens, R.L., Lee, J., Warren, C.D., Jeanloz, R.W., 1984. Structure determination of a tetrasaccharide: transient nuclear Overhauser effects in the rotating frame. J. Am. Chem. Soc. 106, 811–813.
Chalot, M., Brun, A., 1998. Physiology of organic nitrogen acquisition by ectomycorrhizal fungi and ectomycorrhizas. FEMS Microbiol. Rev. 22, 21–44.
Chen, Z., He, W., Beer, M., Megharaj, M., Naidu, R., 2009. Speciation of glyphosate, phosphate and aminomethyl-phosphonic acid in soil extracts by ion chromatography with inductively coupled plasma mass spectrometry with an octopole reaction system. Talanta 78, 852–856.
Chen, S., Liang, Z., Webster, R., Zhang, G., Zhou, Y., Teng, H., et al., 2019. A high-resolution map of soil pH in China made by hybrid modelling of sparse soil data and environmental covariates and its implications for pollution. Sci. Total Environ. 655, 273–283.
Colthup, N., 2012. Introduction to Infrared and Raman Spectroscopy. Elsevier.
Damonte, M., Sánchez, R.M.T., dos Santos Afonso, M., 2007. Some aspects of the glyphosate adsorption on montmorillonite and its calcined form. Appl. Clay Sci. 36, 86–94.
Daouk, S., Frege, C., Blanc, N., Mounier, S., Redon, R., Merdy, P., et al., 2015. Fluorescence spectroscopy to study dissolved organic matter interactions with agrochemicals applied in Swiss vineyards. Environ. Sci. Pollut. Res. 22, 9284–9292.
Day, G.M., Hart, B.T., McKelvie, I.D., Beckett, R., 1997. Influence of natural organic matter on the sorption of biocides onto goethite, II. Glyphosate. Environ. Technol. 18, 781–794.
De Gerónimo, E., Aparicio, V.C., 2022. Changes in soil pH and addition of inorganic phosphate affect glyphosate adsorption in agricultural soil. Eur. J. Soil Sci. 73, e13188.
Delaglio, F., Grzesiek, S., Vuister, G.W., Zhu, G., Pfeifer, J., Bax, A., 1995. NMRPipe: a multidimensional spectral processing system based on UNIX pipes. J. Biomol. NMR 6, 277–293.
Ellert, B., Gregorich, E., 1995. Management-induced changes in the actively cycling fractions of soil organic matter. In: Carbon Forms and Functions in Forest Soils, pp. 119–138.
Franz, J.E., Mao, M.K., Sikorski, J.A., 1997. Glyphosate: A Unique Global Herbicide. American Chemical Society.
Glass, R.L., 1987. Adsorption of glyphosate by soils and clay minerals. J. Agric. Food Chem. 35, 497–500.
Goormaghtigh, E., Ruysschaert, J.-M., Raussens, V., 2006. Evaluation of the information content in infrared spectra for protein secondary structure determination. Biophys. J. 90, 2946–2957.
Hance, R.J., 1976. Adsorption of glyphosate by soils. Pestic. Sci. 7, 363–366.
Hill, P.W., Quilliam, R.S., DeLuca, T.H., Farrar, J., Farrell, M., Roberts, P., et al., 2011. Acquisition and assimilation of nitrogen as peptide-bound and D-enantiomers of amino acids by wheat. PloS One 6, e19220.
Ho, Y.-S., 2006. Review of second-order models for adsorption systems. J. Hazard. Mater. 136, 681–689.
Jan, M., Roberts, P., Tonheim, S., Jones, D., 2009. Protein breakdown represents a major bottleneck in nitrogen cycling in grassland soils. Soil Biol. Biochem. 41, 2272–2282.
Jonsson, C.M., Persson, P., Sjöberg, S., Loring, J.S., 2008. Adsorption of glyphosate on goethite (α-FeOOH): surface complexation modeling combining spectroscopic and adsorption data. Environ. Sci. Technol. 42, 2464–2469.
Kaiser, K., Kalbitz, K., 2012. Cycling downwards–dissolved organic matter in soils. Soil Biol. Bio-chem. 52, 29–32.
Kalbitz, K., Schwesig, D., Rethemeyer, J., Matzner, E., 2005. Stabilization of dissolved organic matter by sorption to the mineral soil. Soil Biol. Biochem. 37, 1319–1331.
Ketterings, Q.M., Reid, W.S., Czymmek, K.J., 2006. Lime Guidelines for Field Crops in New York. Dept. Crop and Soil Sciences Extension Series E06-02.. Cornell Univ, Ithaca, NY.
Khoury, G.A., Gehris, T.C., Tribe, L., Sánchez, R.M.T., dos Santos Afonso, M., 2010. Glyphosate adsorption on montmorillonite: an experimental and theoretical study of surface complexes. Appl. Clay Sci. 50, 167–175.
Kohl, S., Rice, J., 1998. The binding of contaminants to humin: a mass balance. Chemosphere 36, 251–261.
Kolpin, D.W., Thurman, E.M., Lee, E.A., Meyer, M.T., Furlong, E.T., Glassmeyer, S.T., 2006. Urban contributions of glyphosate and its degradate AMPA to streams in the United States. Sci. Total Environ. 354, 191–197.
Ladd, J., Butler, J., 1972. Short-term assays of soil proteolytic enzyme activities using proteins and dipeptide derivatives as substrates. Soil Biol. Biochem. 4, 19–30.
Ladd, M.P., Giannone, R.J., Abraham, P.E., Wullschleger, S.D., Hettich, R.L., 2019. Evaluation of an untargeted nano-liquid chromatography-mass spectrometry approach to expand coverage of low molecular weight dissolved organic matter in Arctic soil. Sci. Rep. 9, 1–13.
Lamiable, A., Thévenet, P., Rey, J., Vavrusa, M., Derreumaux, P., Tufféry, P., 2016. PEP-FOLD3: faster de novo structure prediction for linear peptides in solution and in complex. Nucleic Acids Res. 44, W449–W454.
Li, Y., Sato, T., 2017. Complexation of a globular protein, β-lactoglobulin, with an anionic surfactant in aqueous solution. Langmuir 33, 5491–5498.
Li, W., Wang, Y.-J., Zhu, M., Fan, T.-T., Zhou, D.-M., Phillips, B.L., et al., 2013. Inhibition mechanisms of Zn precipitation on aluminum oxide by glyphosate: a 31P NMR and Zn EXAFS study. Environ. Sci. Technol. 47, 4211–4219.
Li, H., Wallace, A.F., Sun, M., Reardon, P., Jaisi, D.P., 2018. Degradation of glyphosate by Mn-oxide may bypass sarcosine and form glycine directly after C–N bond cleavage. Environ. Sci. Technol. 52, 1109–1117.
Lin, M.-H., Gresshoff, P.M., Ferguson, B.J., 2012. Systemic regulation of soybean nodulation by acidic growth conditions. Plant Physiol. 160, 2028–2039.
Liu, J., Zhang, F., Dou, S., Zhu, M., Ding, L., Yang, Y., 2022. Adsorption of serine at the anatase TiO_2/water interface: a combined ATR-FTIR and DFT study. Sci. Total Environ. 807, 150839.
Mahler, B.J., Van Metre, P.C., Burley, T.E., Loftin, K.A., Meyer, M.T., Nowell, L.H., 2017. Similarities and differences in occurrence and temporal fluctuations in glyphosate and atrazine in small Midwestern streams (USA) during the 2013 growing season. Sci. Total Environ. 579, 149–158.
Mazzei, P., Piccolo, A., 2012. Quantitative evaluation of noncovalent interactions between glyphosate and dissolved humic substances by NMR spectroscopy. Environ. Sci. Technol. 46, 5939–5946.
McBride, M., Kung, K.-H., 1989. Complexation of glyphosate and related ligands with iron (III). Soil Sci. Soc. Am. J. 53, 1668–1673.
McConnell, J.S., Hossner, L.R., 1989. X-ray diffraction and infrared spectroscopic studies of adsorbed glyphosate. J. Agric. Food Chem. 37, 555–560.
Miano, T., Piccolo, A., Celano, G., Senesi, N., 1992. Infrared and fluorescence spectroscopy of glyphosate-humic acid complexes. Sci. Total Environ. 123, 83–92.

Morillo, E., Undabeytia, T., Maqueda, C., 1997. Adsorption of glyphosate on the clay mineral montmorillonite: effect of Cu (II) in solution and adsorbed on the mineral. Environ. Sci. Technol. 31, 3588–3592.
Nelson, D.L., Cox, M.M., 2021. Lehninger Principles of Biochemistry. W.H. Freeman & Company, New York, NY.
Nguyen, T., Kleber, M., Myrold, D.D., 2019. Contribution of different catalytic types of peptidases to soil proteolytic activity. Soil Biol. Biochem. 138, 107578.
Norde, W., 1996. Driving forces for protein adsorption at solid surfaces. In: Macromolecular Symposia, 103. Wiley Online Library, pp. 5–18.
Pal, S., 2019. Fundamentals of Molecular Structural. Academic Press, Biology.
Palafox-Hernandez, J.P., Tang, Z., Hughes, Z.E., Li, Y., Swihart, M.T., Prasad, P.N., et al., 2014. Comparative study of materials-binding peptide interactions with gold and silver surfaces and nanostructures: a thermodynamic basis for biological selectivity of inorganic materials. Chem. Mater. 26, 4960–4969.
Pereira, R.C., Anizelli, P.R., Di Mauro, E., Valezi, D.F., da Costa, A.C.S., Zaia, C.T.B.V., et al., 2019. The effect of pH and ionic strength on the adsorption of glyphosate onto ferrihydrite. Geochem. Trans. 20, 3.
Pessagno, R.C., Dos Santos Afonso, M., Torres Sanchez, R.M., 2005. N-(Phosphonomethyl) glycine interactions with soils. In: Anales de la Asociación Química Argentina, 93. SciELO Argentina, pp. 97–108.
Piccolo, A., Celano, G., 1994. Hydrogen-bonding interactions between the herbicide glyphosate and water-soluble humic substances. Environ. Toxicol. Chem. Int. J. 13, 1737–1741.
Plazinski, W., Rudzinski, W., Plazinska, A., 2009. Theoretical models of sorption kinetics including a surface reaction mechanism: a review. Adv. Colloid Interface Sci. 152, 2–13.
Primost, J.E., Marino, D.J., Aparicio, V.C., Costa, J.L., Carriquiriborde, P., 2017. Glyphosate and AMPA,"pseudo-persistent" pollutants under real-world agricultural management practices in the Mesopotamic Pampas agroecosystem, Argentina. Environ. Pollut. 229, 771–779.
Qualls, R.G., Haines, B.L., Swank, W.T., 1991. Fluxes of dissolved organic nutrients and humic substances in a deciduous forest. Ecology 72, 254–266.
Reardon, P.N., Chacon, S.S., Walter, E.D., Bowden, M.E., Washton, N.M., Kleber, M., 2016. Abiotic protein fragmentation by manganese oxide: implications for a mechanism to supply soil biota with oligopeptides. Environ. Sci. Technol. 50, 3486–3493.
Richards, B.K., Pacenka, S., Meyer, M.T., Dietze, J.E., Schatz, A.L., Teuffer, K., et al., 2018. Antecedent and post-application rain events trigger glyphosate transport from runoff-prone soils. Environ. Sci. Technol. Lett. 5, 249–254.
Roach, P., Farrar, D., Perry, C.C., 2005. Interpretation of protein adsorption: surface-induced conformational changes. J. Am. Chem. Soc. 127, 8168–8173.
Roth, V.-N., Lange, M., Simon, C., Hertkorn, N., Bucher, S., Goodall, T., et al., 2019. Persistence of dissolved organic matter explained by molecular changes during its passage through soil. Nat. Geosci. 12, 755–761.
Russo, F., Johnson, C.J., Johnson, C.J., McKenzie, D., Aiken, J.M., Pedersen, J.A., 2009. Pathogenic prion protein is degraded by a manganese oxide mineral found in soils. J. Gen. Virol. 90, 275–280.
Schmidt, M.P., Martínez, C.E., 2016. Kinetic and conformational insights of protein adsorption onto montmorillonite revealed using in situ ATR-FTIR/2D-COS. Langmuir 32, 7719–7729.
Schmidt, M.P., Martínez, C.E., 2017. Ironing out genes in the environment: an experimental study of the DNA–goethite interface. Langmuir 33, 8525–8532.
Schmidt, M.P., Martínez, C.E., 2018. Supramolecular association impacts biomolecule adsorption onto goethite. Environ. Sci. Technol. 52, 4079–4089.
Schwertmann, U., Cornell, R.M., 2008. Iron Oxides in the Laboratory: Preparation and Characterization. John Wiley & Sons.
Shakiba, S., Hakimian, A., Barco, L.R., Louie, S.M., 2018. Dynamic intermolecular interactions control adsorption from mixtures of natural organic matter and protein onto titanium dioxide nanoparticles. Environ. Sci. Technol. 52, 14158–14168.
Sheals, J., Sjöberg, S., Persson, P., 2002. Adsorption of glyphosate on goethite: molecular characterization of surface complexes. Environ. Sci. Technol. 36, 3090–3095.
Sheals, J., Granström, M., Sjöberg, S., Persson, P., 2003. Coadsorption of Cu(II) and glyphosate at the water–goethite (α-FeOOH) interface: molecular structures from FTIR and EXAFS measurements. J. Colloid Interface Sci. 262, 38–47.
Shoval, S., Yariv, S., 1979. The interaction between roundup (glyphosate) and montmorillonite. Part I. Infrared study of the sorption of glyphosate by montmorillonite. Clay Clay Miner. 27, 19–28.
Skark, C., Zullei-Seibert, N., Schöttler, U., Schlett, C., 1998. The occurrence of glyphosate in surface water. Int. J. Environ. Anal. Chem. 70, 93–104.
Stryer, L., Berg, J., Tymoczko, J., Gatto, G., 2019. Biochemistry. W.H. Freeman & Company, New York, NY.
Sutton, R., Sposito, G., 2005. Molecular structure in soil humic substances: the new view. Environ. Sci. Technol. 39, 9009–9015.
Tamm, L.K., Tatulian, S.A., 1997. Infrared spectroscopy of proteins and peptides in lipid bilayers. Q. Rev. Biophys. 30, 365–429.
Touzeau, J., Seydou, M., Maurel, F., Tallet, L., Mutschler, A., Lavalle, P., et al., 2021. Theoretical and experimental elucidation of the adsorption process of a bioinspired peptide on mineral surfaces. Langmuir 37, 11374–11385.
Tribe, L., Kwon, K.D., Trout, C.C., Kubicki, J.D., 2006. Molecular orbital theory study on surface complex structures of glyphosate on goethite: calculation of vibrational frequencies. Environ. Sci. Technol. 40, 3836–3841.
Undabeytia, T., Morillo, E., Maqueda, C., 2002. FTIR study of glyphosate−copper complexes. J. Agric. Food Chem. 50, 1918–1921.
Van Hees, P.A., Jones, D.L., Finlay, R., Godbold, D.L., Lundström, U.S., 2005. The carbon we do not see—the impact of low molecular weight compounds on carbon dynamics and respiration in forest soils: a review. Soil Biol. Biochem. 37, 1–13.
Vranova, V., Rejsek, K., Formanek, P., 2013. Proteolytic activity in soil: a review. Appl. Soil Ecol. 70, 23–32.
Walsh, T.R., Knecht, M.R., 2017. Biointerface structural effects on the properties and applications of bioinspired peptide-based nanomaterials. Chem. Rev. 117, 12641–12704.
Warren, C., 2021. What are the products of enzymatic cleavage of organic N? Soil Biol. Biochem. 154, 108152.
Wishart, D.S., Sykes, B.D., Richards, F.M., 1992. The chemical shift index: a fast and simple method for the assignment of protein secondary structure through NMR spectroscopy. Biochemistry 31, 1647–1651.
Yan, W., Jing, C., 2018. Molecular insights into glyphosate adsorption to goethite gained from ATR-FTIR, two-dimensional correlation spectroscopy, and DFT study. Environ. Sci. Technol. 52, 1946–1953.
Yang, Y., Schwiderek, S., Grundmeier, G., Keller, A., 2021. Strain-dependent adsorption of *Pseudomonas aeruginosa*-derived adhesin-like peptides at abiotic surfaces. In: Micro, 1. MDPI, pp. 129–139.
Yang, Y., Huang, J., Dornbusch, D., Grundmeier, G., Fahmy, K., Keller, A., et al., 2022. Effect of surface hydrophobicity on the adsorption of a pilus-derived adhesin-like peptide. Langmuir 38, 9257–9265.
Yu, W.H., Li, N., Tong, D.S., Zhou, C.H., Lin, C.X.C., Xu, C.Y., 2013. Adsorption of proteins and nucleic acids on clay minerals and their interactions: a review. Appl. Clay Scie. 80, 443–452.
Zapadka, K.L., Becher, F.J., Gomes dos Santos, A.L., Jackson, S.E., 2017. Factors affecting the physical stability (aggregation) of peptide therapeutics. Interface Focus 7, 20170030.
Zhou, X., Huang, Q., Chen, S., Yu, Z., 2005. Adsorption of the insecticidal protein of Bacillus thuringiensis on montmorillonite, kaolinite, silica, goethite and red soil. Appl. Clay Sci. 30, 87–93.